Experimental Study on Drilling Characteristics of 3D-printed Titanium Alloy

Meng Hu[1,a], Weiwei Ming[1,b], Qinglong An[1,c], Ming Chen[1,d]

[1]School of Mechanical Engineering, Shanghai Jiao Tong University, Shanghai, 200240, P. R. China

[a]humeng@sjtu.edu.cn, [b]mingseas@sjtu.edu.cn, [c]qlan@sjtu.edu.cn, [d]mchen@sjtu.edu.cn

Keywords: 3D-printed Titanium Alloy, Drilling Characteristics, Tool Wear

Abstract. 3D-printed titanium alloy is widely used for producing complex shaped parts, especially for surgery and aerospace. This paper presents the investigation of drilling characteristics of selective laser melted Ti6Al4V titanium alloy. Full factor experiments were carried out with a 6 mm twist drill under dry cutting conditions. The twist drill was coated by AlCrN through PVD process. Drilling force and drilling temperature were measured online. Surface roughness of holes were measured after tests, and tool wear was studied by SEM and EDS. Influences of cutting speed and feed rate on drilling force and drilling temperature were shown and analyzed. Adhesion wear, coating peeling off and abrasive wear were main wear mechanism during drilling of 3D-printed titanium alloy. Surface roughness went up with the increase of feed rate, while cutting speed had a complicated impact on surface roughness.

Introduction

Titanium alloys are widely used in many areas for their high specific strength, good corrosion and high temperature resistance. With the development of additive manufacturing technologies, some complex shape parts can be produced without removing bulk of material and costing too much time. Nowadays, 3D-printed titanium alloys are begun to use in surgery and aerospace fields, such as knee prosthesis, turbine blades and fuel nozzles [1]. Though additive manufacturing aims to reduce the manufacturing steps and the mechanical properties of 3D-printed parts are even better than casted and forged parts, semi-finishing and finishing machining operations are still needed to make the 3D-printed parts meet assembly accuracy requirements, geometrical tolerances and surface quality.

Different additive technologies, such as Selective Laser Melting (SLM), Electron Beam Melting (EBM), Fused Deposition Modeling (FDM), Direct Melting Laser Sintering (DMLS), are used to print near-net-shape titanium parts. In recent years, some works had been focused on the machining of titanium alloys printed by different additive manufacturing technology. Hou et al. [2] optimized milling parameters for milling of SLM Ti6Al4V based on machining quality and process efficiency. Bordin et al. [1, 3] compared performance of cryogenic cooling, dry cutting and wet cutting when turning of EBM Ti6Al4V, cryogenic cooling assured best performance by reducing the tool wear, improving the surface finish and the chip breakability. Sartori et al. [4] investigate the turning performance of DMLS and EBM Ti6Al4V under different cooling strategy, diffusive wear and abrasive wear were significantly reduced under cryogenic cooling. Shunmugavel et al. [5] studied the tool wear and surface integrity during turning of wrought and SLM Ti6Al4V, tool wear and surface quality were worse when tuning of SLM Ti6Al4V. Low cutting speed and feed rate were

recommended for micro-drilling and thread milling of DMLS Ti6Al4V [6]. Oyelola et al. [7] found that the inhomogeneities during additive manufacturing process had a great effect on surface quality of the latter turning process. Higher cutting forces and worse surface roughness were found when turning of SLM Ti6Al4V as compared to wrought Ti6Al4V [8]. Besides experimental studies, Umbrello et al. [9] proposed a FE model to simulate the microstructural variation and hardness change when machining of EBM Ti6Al4V under dry and cryogenic conditions

In this paper, drilling characteristics of SLM Ti6Al4V were investigated. Full factor experiments were carried out with a 6 mm twist drill under dry cutting conditions. Cutting forces and temperatures were measured online. Tool wear mechanism was studied, and influences of drilling parameters were discussed.

Experimental Procedures

The workpiece used in this work was the Ti6Al4V titanium alloy manufactured by Selective Laser Melting (SLM) process. The workpiece was 60mm×60mm×20mm block and prepared by sintering with Ti6Al4V titanium alloy powders. Chemical composition of 3D-printed Ti6Al4V is shown in table 1. Microstructure of 3D-printed titanium alloy is demonstrated in Fig. 1. 3D-printed Ti6Al4V shows a lamellar microstructure, that β phase was acicular and α phase was not equiaxed.

Table 1 Chemical composition of 3D-printed Ti6Al4V [weight, %]

C	N	O	Al	Fe	V	H	Ti
0.04	0.01	0.14	5.79	0.13	4.49	0.002	Bal

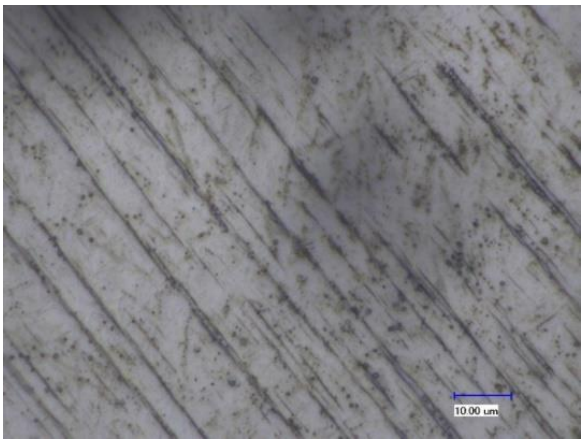

Fig. 1 Microstructure of 3D-printed Ti6Al4V (3000X)

A five-axis machining center (Hurco VMX42) was used for the conduction of the drilling tests. As shown in Fig. 2, a coated cemented carbide twist drill was used as the cutting tool. PVD AlCrN coating was deposited on the twist drill to increase hot hardness and anti-wear of the tool. The coating had a thickness of 4 μm. The twist drill had a diameter of 6mm, helix angle of 30°, edge radius of 0.015mm, chisel edge length of 0.12mm and point angle of 140°.

Fig. 2 Twist drill and its cutting edges

Full factor drilling experiments of 3D-printed Ti6Al4V were carried out under different levels of spindle speed and feed rate. Titanium alloy is known as the hard-to-machine material, so a low spindle speed is recommended in the experiments, whereas the feed rate could be improved properly in consideration of production efficiency. As is shown in table 2, both spindle speed and feed rate are divided into 4 levels separately. Drilling depth of all the experiments is twice the tool diameter, namely 12mm. As thermocouple was embedded at the internal coolant hole of the drill to measure the temperature online, dry cutting was employed in this work.

Table 2 Machining parameters of experiments

Level	1	2	3	4
Spindle speed [r/min]	500	800	1200	1500
Feed rate [mm/rev]	0.06	0.09	0.12	0.15

During the drilling process, drilling force and torque functioned on the workpiece was acquired by a four-dimensional piezoelectric dynamometer online. As mentioned before, thermocouple wires were laid in body of the drill, so that the thermoelectric power could be gained and then be converted to temperature information through the signal analysis equipment. Under every drilling parameter, a new drill was used and 30 holes were drilled to evaluate the tool wear. The tool wear characteristics were analyzed using Scanning Electron Microscope (SEM) and Energy Dispersive Spectrometer (EDS). Besides, surface roughness was also measured by a stylus tester (MitutoyoSJ-201) after drilling.

Experimental Results and Discussions

Tool wear. Fig. 3 shows the SEM pictures of the rake face and flank face of the drill after test under 800 r/min and 0.12 mm/rev. It can be seen that large-area peeling-off of coating exists both on rake face and flank face. This is because the tool's rake face contacts directly with the chip in the cutting process, a strong extrusion and friction force is functioned on the tool's rake face, accompanied by the high cutting temperature, the coating becomes worn down easily. Besides, adhesive phenomenon of small spots of chips is serious on rake face, which is also caused by the strong extrusion force from chips. On the tool's flank face, an obvious feature of abrasive wear could be seen. In addition, micro-chipping also appears at the tool's edge, which could bring hazardous damage to the tool's normal usage in the subsequent machining of 3D-printed Ti6Al4V.

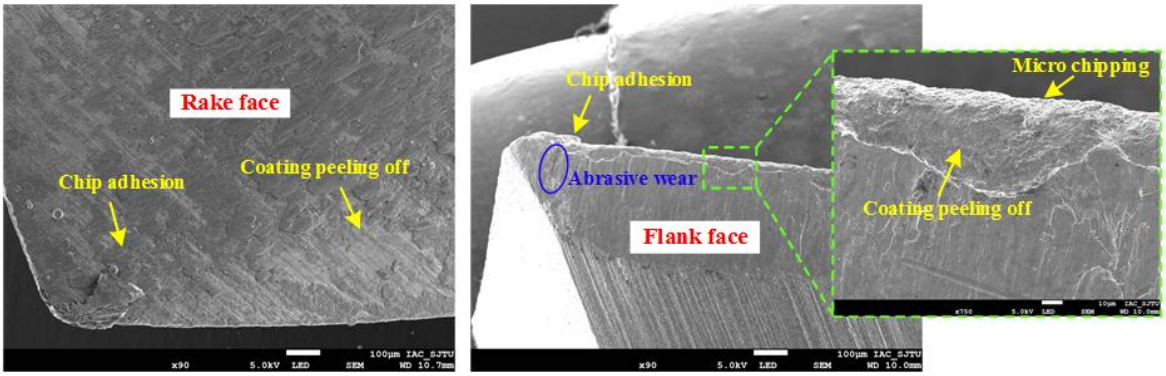

Fig. 3 SEM of the rake face and flank face of the worn tool

With the help of EDS, the chemical elements were analyzed at two small areas chosen from tool's rake face, which are labeled as Area 1 and Area 2 in Fig. 4. In Area 1, the main elements are W, Co and C, indicating that the coating here has been peeled off completely and the tool's substrate material has been exposed on its surface. However, the main elements detected in Area 2 are Ti and Al, meaning that adhesion of titanium alloy exists on the tool's surface.

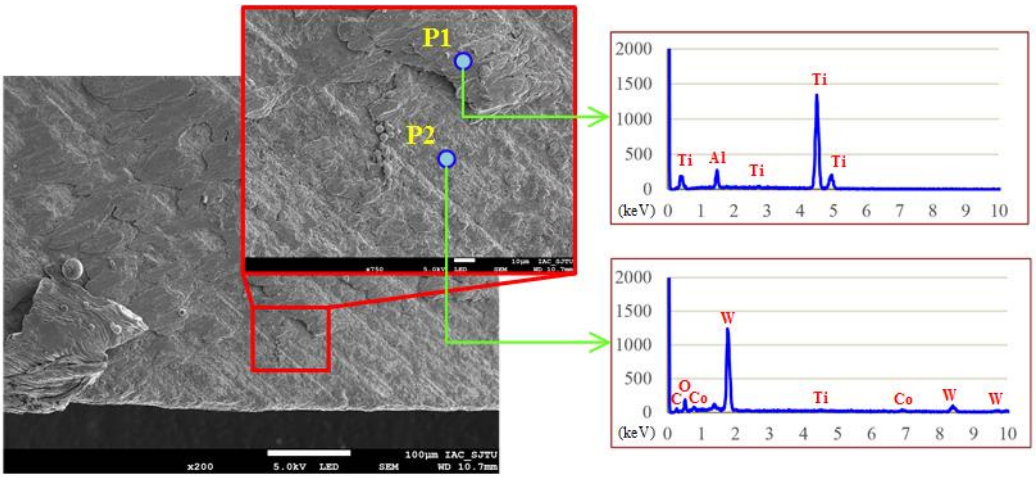

Fig. 4 EDS analysis on tool's rake face

Cutting force. Real-time measurement of the thrust force was performed during the test, after which the acquired data was analyzed statistically, getting results shown in figure 5. It illustrated the effects on thrust forces under different process parameters of spindle speed and feed rate. From figure 5(a), it can be seen that when spindle speed increases from 500 to 1200r/min, thrust force decreases from 525 to 405 N rapidly. While the variation of spindle speed between 1200 r/min and 1500 r/min has almost no influence on thrust force. The reason accounting for this phenomenon may be that with the spindle speed increasing in the initial stage the temperature in drilling area increases gradually, bringing stronger heat softening effect than strain hardening effect. As a result, the flow stress of titanium decreases, causing the thrust force decreasing as well. However, when spindle speed increases continually beyond 1200 r/min, the strain rate hardening effect becomes prominent, balancing well with the heat softening effect. Accordingly, the thrust force keeps unchanged in this stage.

Figure 5(b) shows that the increase of feed rate promotes linear growth of thrust force in machining of 3D-printed titanium alloy. When the drill's feed rate increases, the undeformed chip thickness increases proportionally as well, leading to the increase of shear deformation force of the chip.

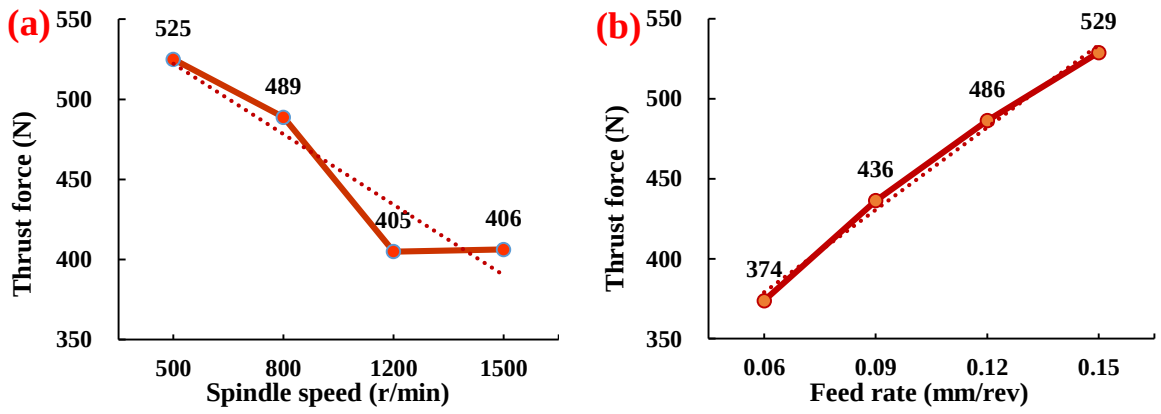

Fig. 5 Thrust forces results of drilling tests: (a) Thrust forces at various cutting speed; (b) Thrust forces at various feed rate

Cutting Temperature. Figure 5 shows the relations of drilling temperature with spindle speed and feed rate respectively. From figure 5(a), the temperature performs nearly linear improvement as the spindle speed increases from 500 to 1500 r/min. It can be explained by the reason that with the

spindle speed increasing, the tool gives more energy to the workpiece material through the drilling force, most of which is then transformed to heat, raising the temperature in cutting zone. Besides, the severer friction between chip and tool's rake face, machined surface and tool's flank face, could also generate more heat to the cutting zone.

From figure 5(b), it can be seen that with the increasing of tool's feed rate from 0.06 to 0.12 mm/rev, drilling temperature increases from 410 to 444 ºC. However, when the feed rate increases from 0.12 to 0.15 mm/rev, drilling temperature drops to 436 ºC. The reason may be that the increasing feed rate could improve the material removal rate, so the drilling force increases as well, which means that more energy will be consumed and transformed to heat, leading to the raising of temperature. When the feed rate increases beyond 0.12 mm/rev, the dissipation of heat distributed in the cutting zone becomes stronger than the generation of heat, causing slight decrease of temperature.

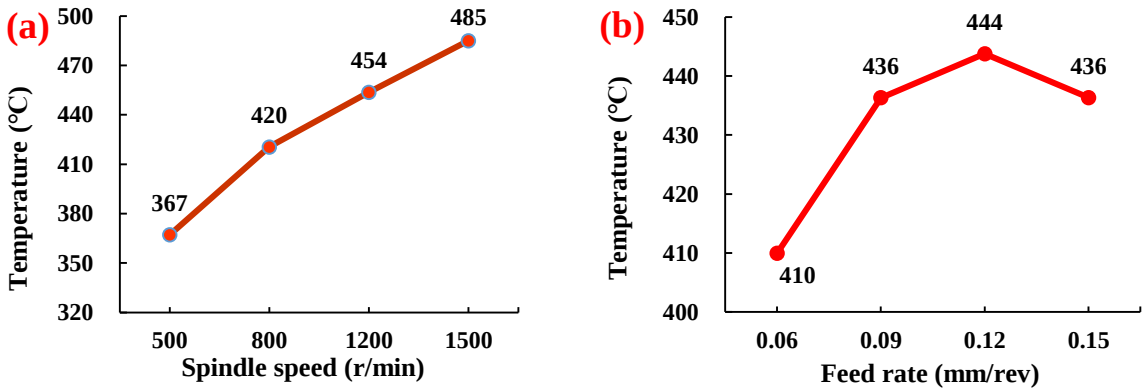

Fig. 6 Drilling temperature results of drilling tests: (a) Drilling temperature at various cutting speed; (b) Drilling temperature at various feed rate

Surface Roughness. After the experiments, holes on the workpiece were sliced into halves along axis direction by electro-spark wire-electrode cutting. Surface of the holes were cleaned by acetone after that. Afterwards, surface roughness was measured by the instrument, as shown in figure 7.

Fig. 7 Measurement of surface roughness of the drilled holes

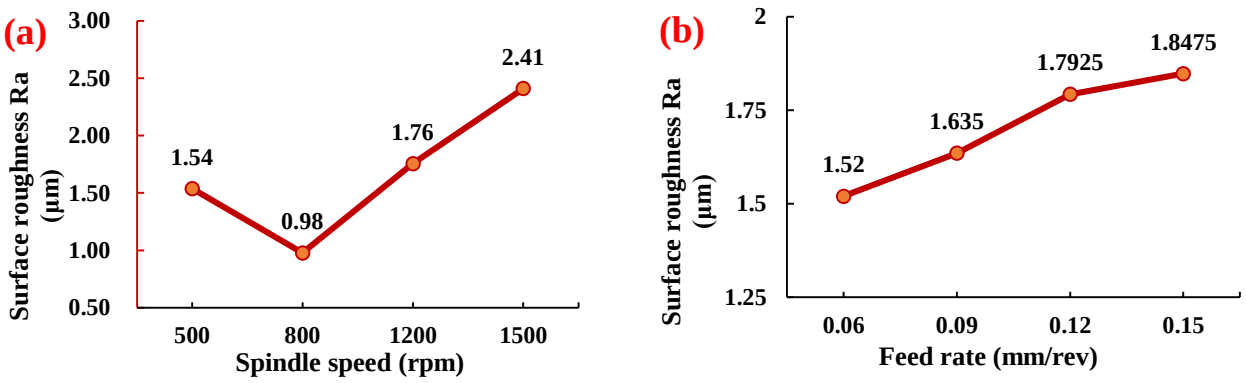

Fig. 8 Surface roughness results of drilling tests: (a) Ra at various cutting speed; (b) Ra at various feed rate

Figure 8 shows the influences on surface roughness under different process parameters of spindle speed and feed rate. It can be seen from figure 8(a) that as spindle speed rises, surface roughness first decreases and then increases. This could be related to the vibration of process system because of the variation of cutting frequency. Severe vibration could deteriorate the quality of machined surface. As for the effect of feed rate on surface roughness, as shown in figure 8(b), it goes up gradually as feed rate increases. The reason could be that the increasing feed rate will generate a bigger drilling force, which can improve the amplitude of vibration, bringing inevitable damage to the machined surface. In addition, with the chip thickness getting bigger, the removal of drilling chip becomes more difficult, which also has bad influence on the machined surface.

Conclusion

Several conclusions can be drawn from the results in drilling of 3D-printed Ti6Al4V using a PVD coated twist drill.

(1) Adhesion wear, coating peeling off and abrasive wear were main wear mechanism during drilling of 3D-printed titanium alloy.

(2) Drilling forces went down with the increase of the cutting speed, and went up with the increase of the feed rate.

(3) Drilling temperature went up with the increase of the cutting speed, and it reached up to 485 ºC at last. Drilling temperature went up before feed rate arrived at 0.12 mm/rev, then the temperature went down when feed rate went beyond 0.12 mm/rev

(4) Surface roughness went up with the increase of feed rate, while cutting speed had a complicated impact on surface roughness. Surface roughness had a close relation to the tool vibration.

Acknowledgment

The work is supported by Important National Science & Technology Specific Projects (2015ZX04002102)

References

[1] A. Bordin, S. Bruschi, A. Ghiotti and P.F. Bariani: Wear, 2015, 328: 89-99.

[2] Y.K. Hou, J.T. Yuan, Z.H. Wang, B.X. Wang: Manufacturing Technology & Machine Tool, 2016 (1): 103-107. (In Chinese)

[3] A. Bordin, S. Sartori, S. Bruschi and A. Ghiotti: Journal of Cleaner Production, 2017, 142, 4142-4151.
[4] S. Sartori, L. Moro, A. Ghiotti and S. Bruschi: Tribology International, 2017, 105: 264-273.
[5] M. Shunmugavel, A. Polishetty, M. Goldberg: International Journal of Materials Forming and Machining Processes (IJMFMP), 2016, 3(2): 50-63.
[6] Z. Rysava, S. Bruschi, S. Carmignato, F. Medeossi, E. Savio and F. Zanini: Procedia CIRP, 2016, 46: 583-586.
[7] O. Oyelola, P. Crawforth, R. M'Saoubi and A.T. Clare: Procedia CIRP, 2016, 45, 119-122.
[8] A. Polishetty, M. Shunmugavel, M. Goldberg, G. Littlefair and R.K. Singh: Procedia Manufacturing, 2017, 7, 284-289.
[9] D. Umbrello, A. Bordin, S. Imbrogno and S. Bruschi: CIRP Journal of Manufacturing Science and Technology, 2017, 18, 92-100.